



## Optimization of combined photocatalytic involving immobilized ZnO nanoparticles and electrochemical processes for ammoniacal nitrogen removal from aqueous solutions

A. Rezaee <sup>a\*</sup>, R. Darvishi Cheshmeh Soltani <sup>a</sup>, A. R. Khataee <sup>b</sup>, H. Godini <sup>c</sup>

<sup>a</sup>Department of Environmental Health, Faculty of Medical Sciences, Tarbiat Modares University, Tehran, Iran

<sup>b</sup>Department of Applied Chemistry, Faculty of Chemistry, University of Tabriz, Tabriz, Iran

<sup>c</sup>Department of Environmental Health, Faculty of Medical Sciences, Khoramabad University, Khoramabad, Iran

Received 29 Apr 2012, Revised 12 June 2012, Accepted 12 June 2012

\* Corresponding author: Abbas Rezaee, E-mail address: [rezaee@modares.ac.ir](mailto:rezaee@modares.ac.ir), Tel/Fax: +982182883575;

### Abstract

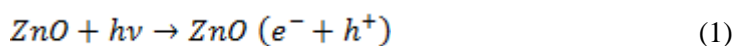
A photocatalytic process consisting of a low-pressure ultraviolet light and ZnO nanoparticles immobilized on glass plates in combination with an electrochemical process using Pt as an anode and graphite as a cathode were used to remove ammoniacal nitrogen from an aqueous solution. A comparison of photocatalytic, electrochemical and combined process for ammoniacal nitrogen removal was performed. The results showed that ammoniacal nitrogen removal follows the increasing order: photocatalytic process < electrochemical process < combined photocatalytic and electrochemical processes. Response surface methodology (RSM) based on central composite design (CCD) was used to evaluate the individual and interactive effects of the four main independent variables, including ammoniacal nitrogen concentration, reaction time, current intensity and initial pH, on the removal of ammoniacal nitrogen. Analysis of variance (ANOVA) exhibited a high coefficient ( $R^2=0.976$  and adjusted  $R^2=0.953$ ), indicating a suitably close fit between the experimental and predicted values. Using a desirability function for the highest ammoniacal nitrogen removal of 76%, the optimum ammoniacal nitrogen concentration, reaction time, current intensity and pH were identified to be 188 mg  $\text{NH}_4\text{-N L}^{-1}$ , 116 min, 664 mA and 6, respectively. Based on the results, the present process can be used as an efficient means for the removal of ammoniacal nitrogen from aqueous media.

**Keywords:** ZnO nanoparticles; Ammoniacal nitrogen; Central composite design; Photocatalysis; Electrochemical process.

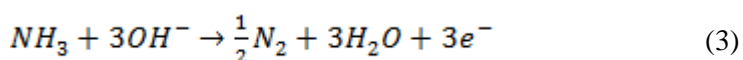
### 1. Introduction

Ammoniacal nitrogen, which is one of the major nitrogen-containing pollutants in wastewater discharged by several industries, has detrimental effects on aqueous environments such as rivers and lakes [1]. This substance can also be emitted from agricultural runoff due to the use of nitrogenous fertilizers on fields [2]. It can cause eutrophication and lead to depletion of dissolved oxygen, which is harmful to aquatic animal life,

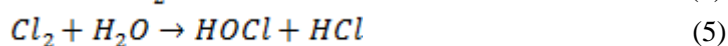
and can also decrease the efficiency of the wastewater disinfection process [3, 4]. Therefore, the removal of ammoniacal nitrogen from wastewater is imperative so as to protect the environment. Several methods have been proposed for ammoniacal nitrogen removal from wastewater, including air and steam stripping, biological nitrification, breakpoint chlorination, ion exchange, and photocatalytic and electrochemical processes [5, 6]. Biological nitrification as an efficient technique for ammoniacal nitrogen removal is limited because of its toxicity, in addition to the high temperature and pH fluctuations in industrial wastewater [1]. The removal of very common nitrogenous pollutants, such as ammoniacal nitrogen, via photocatalytic processes has been reported [1, 7]. Photocatalytic processes can overcome the limitations of existing conventional methods, especially biological nitrification [1]. Among the various catalysts that have been employed in photocatalytic processes,  $\text{TiO}_2$  and  $\text{ZnO}$  are known to be good catalysts for the degradation of several environmental contaminants [8, 9]. Moreover,  $\text{ZnO}$  in the form of nanoparticles, which have a large area-to-volume ratio, exhibit high UV absorption, and have a long life-span, is more effective than  $\text{TiO}_2$  [10]. The toxicity of nanomaterials like  $\text{ZnO}$  nanoparticles for terrestrial and aqueous ecosystems has been demonstrated [11]. Therefore, in the present study,  $\text{ZnO}$  nanoparticles were immobilized on a glass plate surface to mitigate their potentially negative environmental effects and to also make their use more economical. When immobilized  $\text{ZnO}$  is illuminated with UV light, highly reactive electrons and holes are produced, which promote the oxidation of ammoniacal nitrogen [12]. The following reactions demonstrate the formation of the hydroxyl radical ( $\text{OH}^\bullet$ ) via a photocatalytic process using  $\text{ZnO}$  nanoparticles:



The production of  $\text{OH}^\bullet$  can facilitate the oxidation of ammoniacal nitrogen into nitrogen gas in bulk solutions; however, the photocatalytic process has a relatively low efficiency and is time consuming [1]. It has been shown that by using an electrochemical technique and by applying a positive potential through the anode, the efficiency of the photocatalytic process can be improved [12]. A Pt anode electrode is able to oxidize the ammoniacal nitrogen in an electrochemical oxidation process at an acceptable rate [2]. Further, NaCl as a suitable electrolyte in the electrochemical process can also enhance the production of chlorine and hypochlorous acid, which help to oxidize ammoniacal nitrogen to nitrogen gas [13]. The ammonia is adsorbed onto the anode surface and then oxidized by means of an electron transfer reaction:



Initially, in an indirect transformation, oxidants are produced in the reactor by applying a positive potential through the bulk of the reaction solution [12, 13]:



Next, the previously produced chlorine and hypochlorous acid will oxidize ammoniacal nitrogen into nitrogen gas. In addition, the application of UV light at wavelengths ranging from 200 to 400 nm can dissociate hypochlorous acid into hydroxyl radicals  $\text{OH}^\bullet$  and chlorine radicals  $\text{Cl}^\bullet$  [4]:



A combination of the previously described electrochemical process and photocatalytic process for the decolorization of dye solutions has been investigated [14]. Until now, no studies have investigated the degradation of ammoniacal nitrogen via a combined photocatalytic and electrochemical process. Therefore, in the present study, a photocatalytic process consisting of a low-pressure UV light, and immobilized ZnO nanoparticles on glass plates in combination with an electrochemical process using Pt as an anode and graphite as a cathode were used to improve the removal of ammoniacal nitrogen from an aqueous solution. To better evaluate the efficiency of the studied system for ammoniacal nitrogen removal, response surface methodology based on central composite design was used to study the effect of operational parameters, including ammoniacal nitrogen concentration, reaction time, current density and initial pH, on ammoniacal nitrogen removal efficiency due to its advantages in comparison to the traditional “one-at-a-time strategy” [15, 16].

## 2. Experimental

### 2.1. Materials

Ammoniacal water was simulated with deionized water and  $\text{NH}_4\text{Cl}/\text{NaCl}$  that was purchased from Merck, Germany. The concentration of NaCl as the electrolyte was maintained at 0.1 M in all of the experiments. The pH values of the solutions were adjusted using 0.1 M NaOH and 0.1 M  $\text{H}_2\text{SO}_4$ . All other reagents were of analytical grade, except for the NaOH solution that was used to functionalize the surfaces of the glass plates, which was industrial grade.

### 2.2. Immobilization of ZnO nanoparticles on glass plates

ZnO nanoparticles were purchased from US Research Nanomaterials, USA. The ZnO nanoparticles were immobilized on the aforementioned glass plates via the heat attachment method [17]. To functionalize the surfaces of the glass plates (3 cm × 9 cm in size) with hydroxyl groups so as to achieve a better attachment of the ZnO nanoparticles to the plates, concentrated industrial grade NaOH (50%) was used. It has been reported that hydroxyl groups on pretreated glass plates can create covalent or hydrogen bonds between the plate surface and a coated catalyst [16]. After sonication in an ultrasonic bath (Starsonic 18-35, Liarre, Italy) at a frequency of 30 kHz, the sonicated suspension was coated onto the surfaces of the glass plates and then dried in an oven at 90 °C for 1 h. Finally, the ZnO coated glass plates were calcined at 450 °C for 3 h. The amount of ZnO nanoparticles that were successfully coated onto each glass plate surface was determined from the difference in weight of the glass plates before and after the coating process. The amount on ZnO that was successfully coated onto the plate surfaces was approximately  $1.5 \pm 0.17 \text{ mg cm}^{-2}$ .

### 2.3. Combined photocatalytic and electrochemical system

The treatment process was carried out in a 500-mL cylindrical glass cell reactor. The reactor was equipped with a Pt (1 cm wide, 5 cm long and 0.2 cm thickness) anode and graphite (2.5 cm wide, 7 cm long and 0.5 cm thickness) as a porous cathode. It has been reported that a 2-electrode configuration reactor without a reference electrode is as effective as a 3-electrode configuration reactor [12]. A 6-W low-pressure mercury vapor lamp (Cathodeon, UK) was placed in the center of the reactor. Four glass plates that had been previously coated with ZnO nanoparticles were located peripherally in the reactor. Figure 1 depicts a schematic flow diagram of the batch mode experimental reactor. To keep the temperature of the reactor at 25 °C, the reactor was covered with a circulating water jacket. Before each experiment, the reactor was placed in the dark and the solution containing ammoniacal nitrogen was circulated through the reactor until adsorption equilibrium was reached. In all experiments carried out in the present work, loss of ammoniacal nitrogen due to the adsorption on the surface of catalyst was negligible.

### 2.4. Analytical methods

The pH of the solution was measured via a pH meter (Jenway 3505, UK). Ammoniacal nitrogen ( $\text{NH}_4\text{-N}$ ), nitrate ( $\text{NO}_3\text{-N}$ ), nitrite ( $\text{NO}_2\text{-N}$ ) were colorimetrically measured with a UV-Vis spectrophotometer (Unico

2100). The total Kjeldahl nitrogen (TKN) contents were determined according to standard methods for the examination of water and wastewater. The total nitrogen (TN) content is composed of organic nitrogen, ammonium, nitrate and nitrite, whereas the total Kjeldahl nitrogen (TKN) content is the sum of the organic nitrogen and ammonium components; therefore, the total nitrogen (TN) content can be calculated as the sum of oxidized nitrogen (nitrate and nitrite) and TKN [18]. The removal efficiency of ammoniacal nitrogen (%) was calculating using the following expression:

$$\text{Removal efficiency (\%)} = \left(1 - \frac{C}{C_0}\right) \times 100 \quad (7)$$

where  $C_0$  and  $C$  are the ammoniacal nitrogen concentrations at time 0 and  $t$ , respectively. Scanning electron microscopy (SEM) (Philips XL 30, the Netherlands) was used to analyze the surface morphology of the ZnO nanoparticle coatings on the glass plates. SEM images were further supported by energy dispersive X-ray (EDX) microanalysis, which was conducted at an acceleration voltage of 30 kV. EDX provides direct evidence for the purity, existence and distribution of specific elements in a nanocatalyst solid sample. The crystalline phase and solid structure of the ZnO nanoparticles were analyzed using X-ray diffraction (XRD) (Siemens D5000, Germany). The peaks of the XRD indicates the nature of the nanoparticles [19].

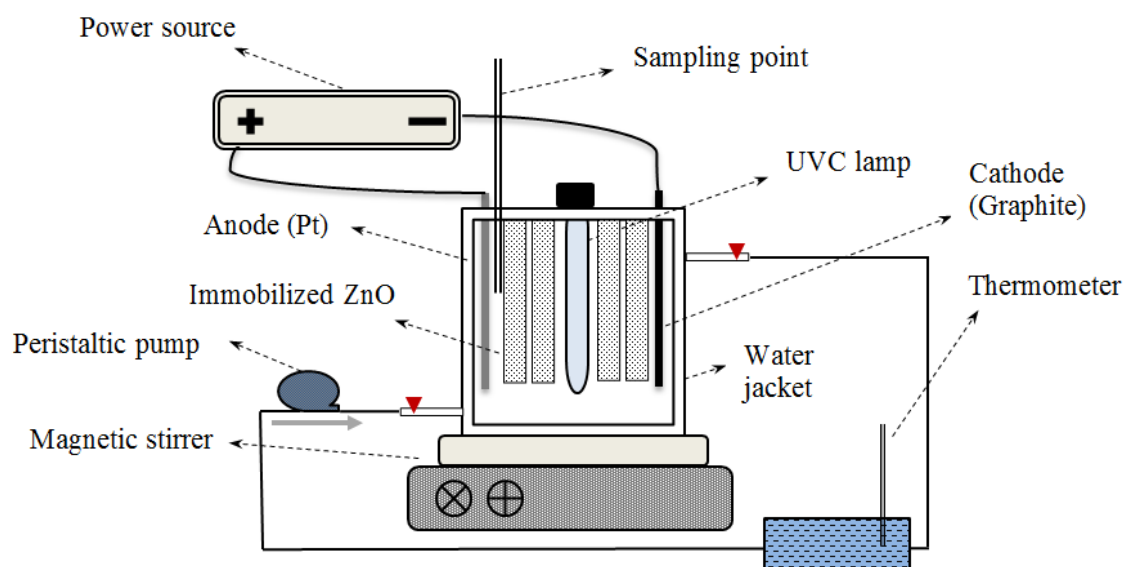


Figure 1. A schematic flow diagram of the experimental reactor.

### 2.5. Experimental design

CCD was conducted to optimize the ammoniacal nitrogen removal efficiency. The primary objective of CCD is to optimize the response surface, which is influenced by other variables in the experiment. To evaluate the effect of other variables on the ammoniacal nitrogen removal efficiency, four main factors (variables) were selected: the initial ammoniacal nitrogen concentration ( $\text{mg NH}_4\text{-N L}^{-1}$ ), reaction time (min), current intensity (mA) and initial pH. The number of required experimental runs was calculated using the following equation:

$$N = 2^k + 2k + x_0 \quad (8)$$

where N is the number of required experimental runs (fact), k is the number of variables and  $x_0$  (axial) is the number of central points. Thus, according to the previous equation, for this design, the total number of required experimental runs is 30 ( $k=4$ ,  $x_0=6$ ). Minitab 16 and Design-Expert 7.0 software were used for the regression and graphical analyses of the obtained experimental data. The variables  $X_i$  were coded as  $x_i$  for statistical analysis according to the following equation:

$$x_i = \frac{X_i - X_0}{\delta X} \quad (9)$$

where  $X_0$  and  $\delta X$  are the values of  $X_i$  at the center point and step change, respectively. The experimental ranges of the variables concerning ammoniacal nitrogen removal are summarized in Table 1. The studied process can be described by the following empirical second-order polynomial model:

$$Y = b_0 + \sum_{i=1}^n b_i x_i + (\sum_{i=1}^n b_{ii} x_i)^2 + \sum_{i=1}^{n-1} \sum_{j=i+1}^n b_{ij} x_i x_j \quad (10)$$

where Y is the predicted response and is the dependent variable (ammoniacal nitrogen removal efficiency),  $b_0$  is a coefficient constant,  $b_i$  are linear coefficients,  $b_{ij}$  are interaction coefficients and  $b_{ii}$  are quadratic coefficients. Moreover,  $x_i$  and  $x_j$  are the coded values for the experimental variables.

Table 1. Ranges and levels of the experimental variables.

variables	Ranges and levels				
	$-\alpha$	-1	0	+1	$+\alpha$
Initial ammoniacal nitrogen concentration (mg L <sup>-1</sup> NH <sub>4</sub> -N)	100	150	200	250	300
Reaction time (min)	10	37.5	65	92.5	120
Current intensity (mA)	140	280	420	560	700
Initial pH	3	4.5	6	7.5	9

### 3. Results and discussion

#### 3.1. The effect of combining photocatalytic and electrochemical processes

A comparison of photocatalytic, electrochemical and combined photocatalytic and electrochemical processes for ammoniacal nitrogen removal from aqueous solution was performed. The removal efficiency of the studied processes for 100 mg NH<sub>4</sub>-N L<sup>-1</sup> as initial ammoniacal nitrogen concentration under electrolysis at 700 mA and initial NaCl concentration of 0.1 M during 90 min at neutral pH was compared according to Figure 2. It can be observed that the highest ammoniacal nitrogen removal was obtained using combined photocatalytic and electrochemical processes. The ammoniacal nitrogen removal during 90 min of combined process was 96.3%, whereas at the same time, electrochemical and photocatalytic processes led to 68.55% and 13.10% of ammoniacal nitrogen removal efficiency, respectively. The results show that the combination of photocatalytic process with electrochemical process can synergistically increase the ammoniacal nitrogen removal efficiency. This finding can be explained by the mentioned mechanisms (Eqs, 1-6) in the introduction section. It was shown that the application of UVC light can facilitate ammonium oxidation as a result of photolysis of the hypochlorous acid produced into  $OH^\bullet$  and  $Cl^\bullet$  (Eq. 6). Kropp and colleagues found that by using an electrochemical technique, the efficiency of the photocatalytic process for removing ammoniacal nitrogen can be improved [12].

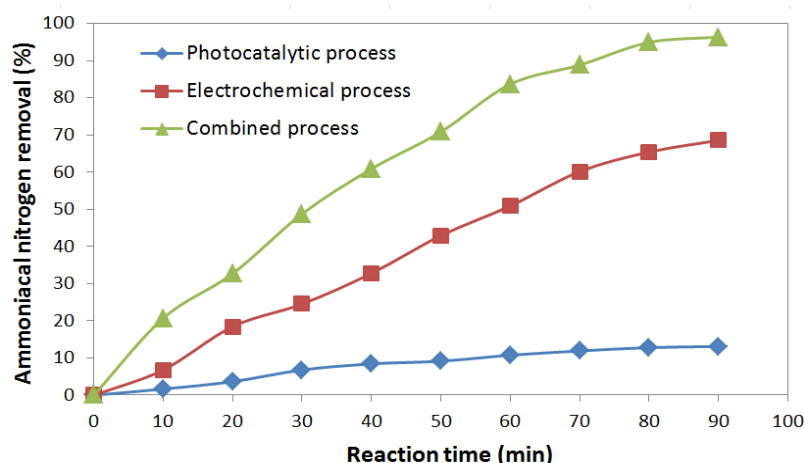


Figure 2. Ammoniacal nitrogen removal (%) by means of different studied processes as the function of reaction time. Initial ammoniacal nitrogen concentration = 100 mg NH<sub>4</sub>-N L<sup>-1</sup>, current intensity = 700 mA, reaction time = 90 min, [NaCl] = 0.1 M and pH = neutral.

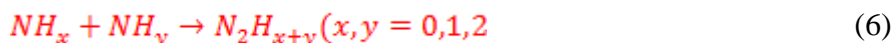
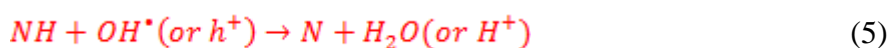
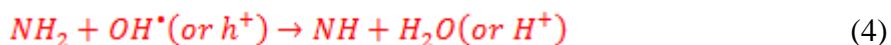
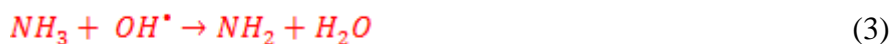
### 3.2. Characteristics of immobilized ZnO nanoparticles on glass plates

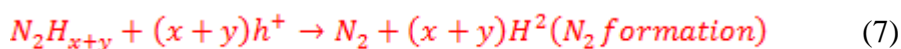
Figure 3<sub>a</sub> depicts the surface structure of the ZnO nanoparticles. The obtained micrographs demonstrate that the ZnO nanoparticles have a good porosity and uniform size [Figure 3<sub>a</sub>]. A relatively equal distribution of the ZnO nanoparticles coated on the glass plate can be seen [Figure 3<sub>b</sub>]. In Figure 3<sub>c</sub> and <sub>d</sub>, the EDX microanalysis and XRD patterns of the ZnO nanoparticles are shown, respectively. Based on the EDX analysis, an associated quantitative analysis of the ZnO nanoparticles demonstrated that the catalyst was highly pure, at 100 wt%. Moreover, the EDX spectrum of the ZnO nanoparticles depicted the presence of several Zn peaks, confirming the original nature of the catalyst [Figure 3<sub>c</sub>]. The peaks of the XRD patterns of the ZnO nanoparticles are quite sharp, indicating the crystalline nature of the nanoparticles. No other peaks corresponding to secondary ZnO phases or impurities were observed, suggesting that the ZnO nanoparticles were highly pure [Figure 3<sub>d</sub>].

### 3.3. Conversion of the ammoniacal nitrogen via the investigated process

The rates of formation of nitrate and nitrite during the combined photocatalytic and electrochemical process at different ammoniacal nitrogen concentrations were investigated, wherein the formation of negligible nitrate and nitrite concentrations at different ammoniacal nitrogen concentrations can be observed. The reason of this observation is thought to derive from the fact that chlorine, hypochlorous acid and the radicals produced within the electrolyte (*OH*<sup>•</sup> and *Cl*<sup>•</sup>) can oxidize ammoniacal nitrogen into nitrogen gas. The *OH*<sup>•</sup> produced can facilitate the oxidation of ammoniacal nitrogen into nitrogen gas or nitrite and nitrate ions in bulk aqueous solution via the following two pathways [1].

Pathway (I):





Pathway (II):



To provide evidence of this assertion, the sum of the remaining ammoniacal nitrogen in the solution, nitrate and nitrite should be approximately equal to the total nitrogen (TN) that remains after each experiment, which would indicate that there are no intermediates in the solution [4]. At an initial ammoniacal nitrogen concentration of 300 mg NH<sub>4</sub>-N L<sup>-1</sup>, approximately 182.02 mg N L<sup>-1</sup> remained in the solution, which was approximately equal to the sum of the remaining ammoniacal nitrogen at 165.65 mg NH<sub>4</sub>-N L<sup>-1</sup>, NO<sub>3</sub>-N at 13.16 mg L<sup>-1</sup> and NO<sub>2</sub>-N at 0.00 mg L<sup>-1</sup>.

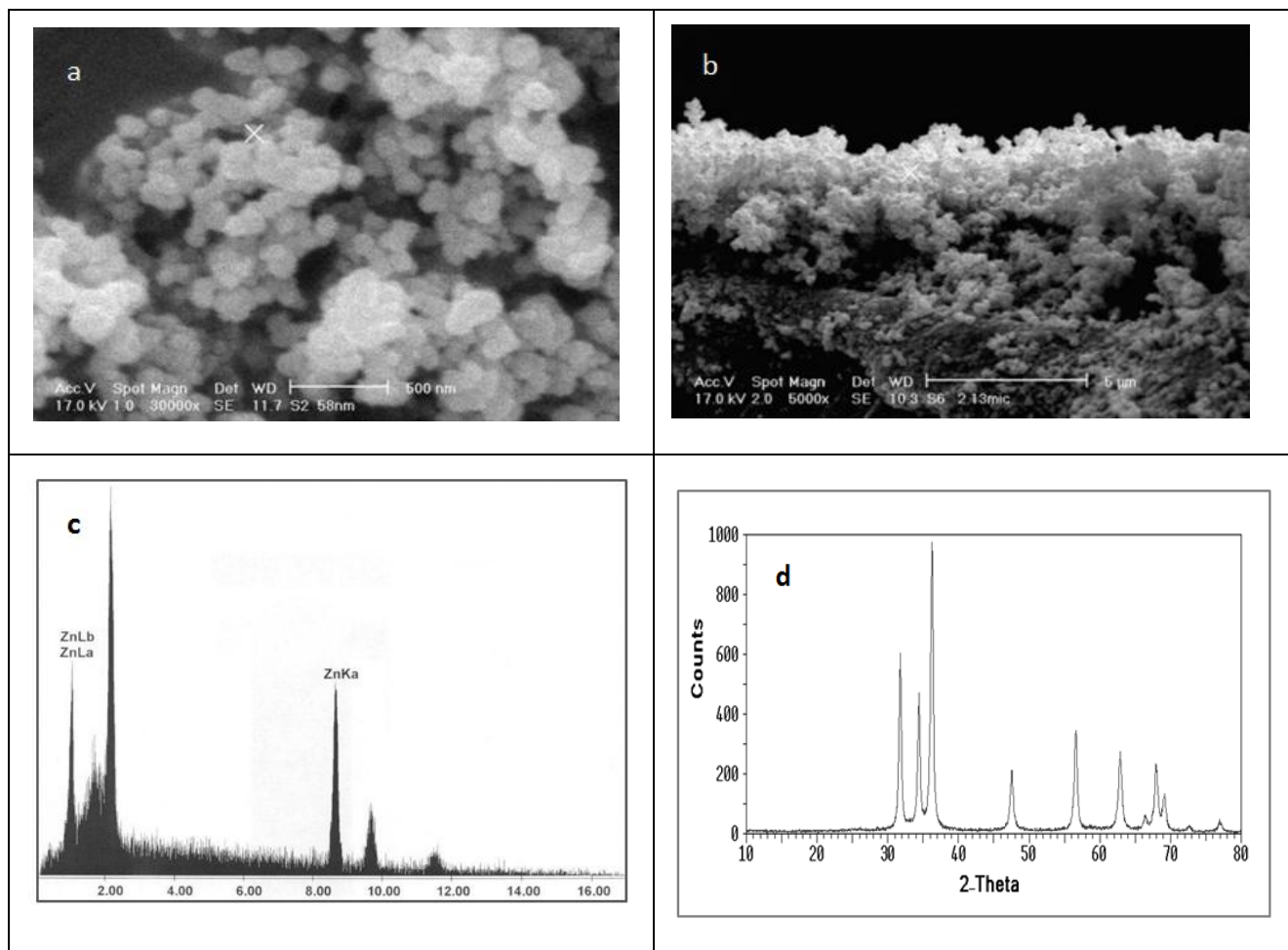


**Figure 3.** Scanning electron microscopy (SEM) images of (a) the ZnO nanoparticles at 30,000X magnification and (b) ZnO nanoparticles that were coated on glass plate surfaces at 5,000X magnification. (c) Energy dispersive X-ray (EDX) microanalysis and (d) X-ray diffraction (XRD) patterns of the ZnO nanoparticles.

### 3.4. CCD model results for ammoniacal nitrogen removal

Using the CCD model, the following second-order polynomial quadratic response equation was used to establish a mutual relationship between the studied variables:

$$Y = b_0 + b_1x_1 + b_2x_2 + b_3x_3 + b_4x_4 + b_{12}x_1x_2 + b_{13}x_1x_3 + b_{14}x_1x_4 + b_{23}x_2x_3 + b_{24}x_2x_4 + b_{34}x_3x_4 + b_{11}x_1^2 + b_{22}x_2^2 + b_{33}x_3^2 + b_{44}x_4^2 \quad (18)$$

where Y is the response factor of the ammoniacal nitrogen removal efficiency (%).  $b_i$ ,  $b_{ii}$ ,  $b_{ik}$  and  $x_i$  are regression coefficients for linear effects, regression coefficients for squared effects, regression coefficients for interaction effects and the coded experimental levels of the variables, respectively. The predicted values of the response were obtained via quadratic model fitting methods using Design-Expert software. An empirical mutual relationship between the response dependent variable and independent variables was established according to the below equation:

$$Y \text{ (ammoniacal nitrogen removal \%)} = 43.61 - 4.82 x_1 + 5.40 x_2 + 9.04 x_3 - 1.76 x_4 - 1.84 x_1x_2 - 0.93 x_1x_3 + 0.027 x_1x_4 + 3.12 x_2x_3 - 4.39 x_2x_4 + 0.30 x_3x_4 + 0.77 x_1^2 - 1.06 x_2^2 - 0.67 x_3^2 + 1.52 x_4^2 \quad (19)$$

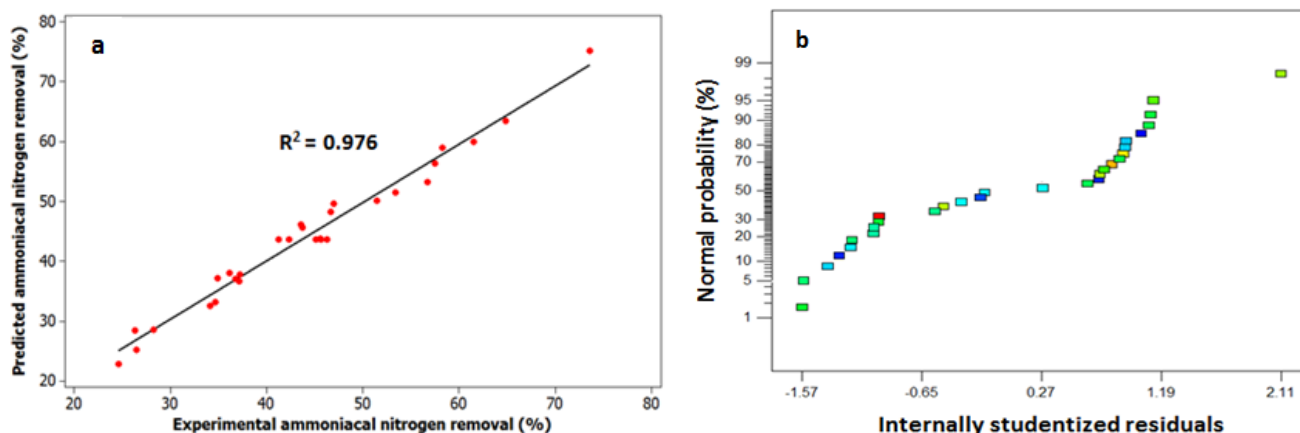
The statistical significance of the quadratic model was assessed by an analysis of variance (ANOVA). The Utilizing ANOVA is useful to evaluate the suitability and significance of the studied model. Table 2 demonstrates that the regression model has a high coefficient of determination ( $R^2=0.976$ ), indicating that 97.6% of the variations of ammoniacal nitrogen removal can be explained by the independent variables.

**Table 2.** Analysis of variance (ANOVA) for ammoniacal nitrogen removal.

Source of variations	Sum of squares	Degree of freedom	Mean square	F-value	P-value (Probe > F)
Regression	3963.43	14	283.46	42.77	0.0001
Residuals	99.40	15	6.63		
Lack of Fit	73.09	10	7.31	1.39	0.3767
Pure Error	26.31	5	5.26		
Total	4067.84	29			

$R^2=0.976$ , adjusted  $R^2=0.953$ , predicted  $R^2=0.887$ , adeq precision=28.75 and CV=5.84%

In fact, the model fails to explain only 2.4% of the variation. The value of the adjusted  $R^2$  ( $R^2=0.953$ ) also demonstrates the significance of the model. Moreover, the predicted  $R^2$  of 0.887 reasonably agrees with the adjusted  $R^2$  of 0.953. The P-values can also be used as a tool to check the significance of the results. It is important to note that “Adeq precision” measures the difference between the signal and noise (signal-to-noise ratio), and a ratio of greater than 4 is favorable. According to Table 2, the obtained ratio of 28.75 indicates an adequate signal. In addition, a low value of the coefficient of variation (CV = 5.84%) indicates a relatively good reliability for the experiments that were carried out for the removal of ammoniacal nitrogen via the studied process. An adequacy check of the applied model is an important part of the experimental analysis. A suitable model can ensure an excellent estimation of real conditions. In order to evaluate the adequacy of the model, experimental and predicted data were compared, as depicted in Figure 4<sub>a</sub>. The Figure demonstrates a good agreement between the predicted ammoniacal nitrogen removal percent and the actual obtained value ( $R^2=0.976$ ).



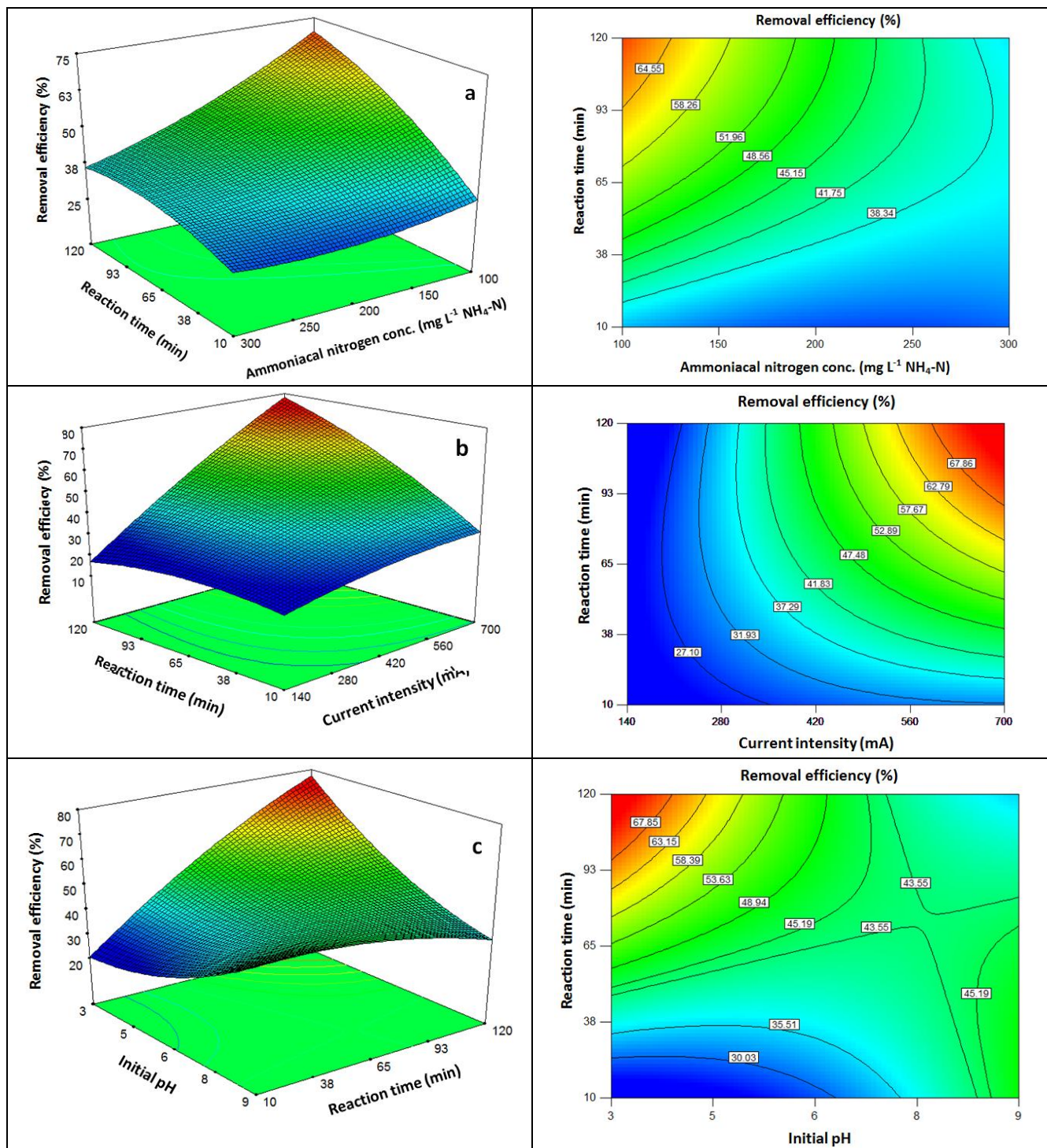
**Figure 4.** The plots of (a) the actual experimental data versus the predicted values and (b) the normal % probability versus the internally studentized residuals for the removal of ammoniacal nitrogen.

Figure 4<sub>b</sub> depicts the internally studentized residuals and normal probability (%) plot for ammoniacal nitrogen removal. As depicted in Figure 4<sub>b</sub>, the obtained data points consistently appear on a straight trend line, demonstrating that there is no obvious dispersal.

### 3.5. Interactive influences of independent variables

Response surface plots can be applied for various interactions of any two variables. These plots can be used to assess any changes in the response surface based on a polynomial function. In this approach, two variables are constant and the other two variables will be varied within the experimental ranges. The effect of the initial ammoniacal nitrogen concentration on ammoniacal nitrogen removal efficiency is depicted in Figure 5 (a).

The removal efficiency increased as a function of decreasing initial ammoniacal nitrogen. It can be stated that as the initial concentration of the ammoniacal nitrogen decreases, more radicals ( $OH^{\bullet}$  and  $Cl^{\bullet}$ ) are available to remove the ammoniacal nitrogen, such that the removal efficiency increases. The removal efficiency (%) of ammoniacal nitrogen as a function of current intensity is illustrated in Figure 5 (b). As can be seen, the highest removal efficiency at constant pH and ammoniacal nitrogen concentration values is up to 70% when the current intensity and reaction time reach 700 mA and 120 min, respectively. This demonstrates increasing removal efficiency as a function of increasing reaction time and current intensity. Increasing the potential applied to the electrodes can accelerate the separation of electron-hole pairs and create significantly more  $OH^{\bullet}$  and  $Cl^{\bullet}$  radicals, leading to increased ammoniacal nitrogen removal [16]. Figure 5<sub>c</sub> depicts the effect of the initial pH on the ammoniacal nitrogen removal efficiency. As shown in Figure 5<sub>c</sub>, the ammoniacal nitrogen removal efficiency increases with increasing initial pH at short exposure times; however, at higher exposure times up to 60 min, the ammoniacal nitrogen removal efficiency increased with decreasing initial pH. First of all, it can be stated that ammoniacal nitrogen removal does not occur at the anode surface but is, instead, mediated by a soluble intermediary, as ammoniacal nitrogen oxidation at the anode surface occurs under basic conditions due to positively charged  $NH_4^+$  in an acidic solution [12].



**Figure 5.** Response surface plots and their corresponding counter plots of ammoniacal nitrogen removal efficiency (%) as the function of (a) initial ammoniacal nitrogen concentration, (b) current density and (c) initial pH. Reaction time = 10-120 min.

Therefore, ammoniacal nitrogen removal will be accomplished in the bulk of the solution. Considering this fact, ammoniacal nitrogen removal at higher pH values can be supported by increasing the oxidation potential of the produced radicals via increasing the reaction time [37]. Totally, it can be stated that the ammoniacal nitrogen removal by the studied process is independent of the initial pH. In agreement with this study, in another study, it has been shown that varying the pH value between 5 and 10 has no impact on the aqueous ammonia removal efficiency using photoelectrocatalytic oxidation [12].

### 3.6. Optimization using the desirability function

By using numerical optimization, a desirable value for each input factor and response can be selected. Therein, the possible input optimizations that can be selected include: the range, maximum, minimum, target, none (for responses) and set so as to establish an optimized output value for a given set of conditions. In the case of a recent study, the input variables were given specific ranged values, whereas the response was designed to achieve a maximum. Using these conditions, the maximum achieved ammoniacal nitrogen removal efficiency was 76% at an initial pH of 6, ammoniacal nitrogen concentration of 188 mg NH<sub>4</sub>-N L<sup>-1</sup>, reaction time of 116 min and current intensity of 664 mA. The confirmatory experiment showed an ammoniacal nitrogen removal efficiency of 74.78% under optimal conditions compared with the ammoniacal nitrogen removal percent of 76% obtained by the model. This indicates the suitability and accuracy of the model.

### Conclusions

In the present study, the removal of ammoniacal nitrogen from aqueous solutions has been studied via a combined electrochemical and photocatalytic process in the context of RSM. Analyses of the response surfaces were carried out as a function of the initial ammoniacal nitrogen concentration, reaction time, current intensity and initial pH. ANOVA demonstrated a high coefficient of determination ( $R^2=0.976$ ), thereby indicating a satisfactory fit between the second order regression model and the experimental results. Optimal conditions, which yielded a maximized ammoniacal nitrogen removal of 76%, were identified using RSM with Design-Expert software, which included an initial pH of 6, ammoniacal nitrogen concentration of 188 mg NH<sub>4</sub>-N L<sup>-1</sup>, reaction time of 116 min and current intensity of 664 mA. It is concluded that the present process can be used as an efficient means for the removal of ammoniacal nitrogen from wastewater. However, based on the results, the electrochemical process is much more efficient than photocatalytic process to oxidize ammoniacal nitrogen. Moreover, RSM was a suitable method to optimize the operational parameters and maximize the ammoniacal nitrogen removal efficiency.

### Acknowledgement

The authors thank Tarbiat Modares University for their instrumental and financial support.

### References

1. Pretzer, L. A., Carlson P. J., Boyd J. E. J.E, *J. Photochem. Photobiol. Chem.* 200 (2008) 246-253.
2. Bonnin E.P., E.J. Biddinger, G.G. Botte, *J. Power. Sourc.* 182 (2008) 284-290.
3. Kim K.-W., Y.-J. Kim, I.-T. Kim, G. Park, II, E.-H. Lee, *Water Res.* 40 (2006), 1431-1441.
4. Xiao S., J. Qu, X. Zhao, H. Liu, D. Wan, *Water. Res.* 43 (2009), 1432-1440.
5. Ou H.-H., M.R. Hoffmann, C.-H. Liao, J.-H. Hong, S.-L. Lo, *Appl. Catal. B: Environ.* 99 (2010), 74-80.
6. Kim K.-W., Y.-J. Kim, I.-T. Kim, G.-I. Park, E.-H. Lee, *Electrochim. Acta.* 50 (2005), 4356-4364.
7. Liu L.-F., Y. Zhang, F.-L. Yang, G. Chen, J.C. Yu, *Separ. Purif. Tech.* 67 (2009), 244-248.
8. Liu H.-L., T.C.-K. Yang, *Process. Biochem.* 39 (2003), 475-481.
9. Rezaee A., M.T. Ghaneian, N. Taghavinia, M.K. Aminian, S.J. Hashemian, *Environ. Tech.* 30 (2009), 233-239.

10. Hong R.Y., J.H. Li, L.L. Chen, D.Q. Liu, H.Z. Li, Y. Zheng, J. Ding, *Powder. Tech.* 189 (2009), 426–432.
11. Peralta-Videa J.R., L. Zhao, M.L. Lopez-Moreno, G. de la Rosa, J. Hong, J.L. Gardea-Torresdey, *J. Hazard. Mater.* 186 (2011), 1-15.
12. Kropp R., D. Tompkins, T. Barry, W. Zeltner, G. Pepping, M. Anderson, T. Barry, *Aquacult. Eng.* 41 (2009), 28-34.
13. Zhang H., X. Ran, X. Wu, D. Zhang, *J. Hazard. Mater.* 188 (2011), pp. 261-268.
14. Khataee A.R., M. Zarei, S.K. Asl, *J. Electroanal. Chem.* 648 (2010), 143-150.
15. Cho I.-H., K.-D. Zoh, *Dyes. Pigments.* 75 (2007), 533-543.
16. Fu J., Y. Zhao, Q. Wu, *J. Hazard. Mater.* 144 (2007), 499-505.
17. Behnajady M.A., N. Modirshahla, M. Mirzamohammady, B. Vahid, B. Behnajady, *J. Hazard. Mater.* 160 (2008), 508-513.
18. APHA, AWWA, WEF, *Standard methods for the examination of water and wastewater*, American Public Health Association, 20<sup>th</sup> edition, Washington DC, (1999).
19. Sivalingam G., Madras G., *Int. Eng. Chem. Res.* 41 (2002), 5337-5340.

(2012), [www.jmaterenvirosnci.com](http://www.jmaterenvirosnci.com)